Title
Human Perivascular Stem Cells and Nel-like protein-1 Synergistically Enhance Spinal Fusion in Osteoporotic Rats

Author
Girgius, Caroline

Publication Date
2016

Peer reviewed|Thesis/dissertation

UNIVERSITY OF CALIFORNIA

Los Angeles

Human Perivascular Stem Cells and Nel-like protein-1 Synergistically Enhance Spinal Fusion in Osteoporotic Rats

A dissertation submitted in partial satisfaction of the requirements

for the degree of Master's of Science in Oral Biology

By

Caroline Magdy Mikhael Girgius

2016

ABSTRACT OF THE THESIS

Human Perivascular Stem Cells and

Nel-Like Protein-1 Synergistically Enhance Spinal

Fusion in Osteoporotic Rats

By

Caroline Magdy Mikhael Girgius

Master's of Science in Oral Biology

University of California, Los Angeles, 2016

Professor Kang Ting, Chair

One of the many complications of osteoporosis is compromised biomechanical integrity of the spine and fractures. Spinal fusion, is a common surgical procedure for osteoporotic patients. As bone formation is a coupled process between osteoblasts and osteoclasts maintaining homeostasis within bone, resorptive agents that induce osteoclasts apoptosis might not be effective in spinal fusion surgeries, for example bisphosphonates, which necessitates new bone formation. Therefore, autologous bone is the standard grafting procedure. However, these grafts are limited in quantity and include donor-site morbidity. Thus, there is a need for stem cell based spinal fusion therapy with proven efficacy. We purified a population of mesenchymal stem cell (MSC) termed perivascular stem cells (PSCs) from adipose tissue using fluorescence-activated cell sorting. The

purified PSCs contain pericytes and adventitial cells that retains the same properties of cultured MSCs. Our studies showed that human perivascular stem cells (hPSCs) exhibit osteogenic potential resulting in robust bone formation in spinal fusion procedures on healthy rats. The aim of this study is to determine the efficacy of hPSCs in the presence and absence of NELL-1, an osteogenic protein, for spinal fusion under osteoporotic conditions. Osteogenic differentiation of hPSCs with and without NELL-1 was tested *in vitro*. The results indicated that NELL-1 significantly increased the osteogenic potential of hPSCs in both osteoporotic and non-osteoporotic donors. Next, spinal fusion was performed by implanting scaffolds with regular or high doses of hPSCs, with or without NELL-1 in ovariectomized rats (n=41). Regular doses of hPSCs or NELL-1 achieved the fusion rates of only 20-37.5% by manual palpation. These regular doses had previously been shown to be effective in non-osteoporotic rat spinal fusion. Remarkably, the high dose of hPSCs+NELL-1 significantly improved the fusion rates among osteoporotic rats up to ~83.3%. Micro-CT quantification confirmed solid bony fusion with high dose hPSCs+NELL-1. Finally, histologically, direct in situ involvement of hPSCs in ossification was shown using un-decalcified samples. To conclude, hPSCs combined with NELL-1 has great potential as a novel therapeutic strategy for osteoporotic patients.

Keywords

Spinal fusion. Osteoporosis. Perivascular stem cell. NEL-like protein-1.

The thesis of Caroline Magdy Mikhael Girgius is approved by

Xinli Zhang, Adjunct Professor

Shen Hu, Associate Professor

Reuben Han-Kyu Kim, Associate Professor

Kang Ting, Professor, Committee Chair

University of California, Los Angeles

2016

TABLE OF CONTENTS

TABLE OF CONTENTS (CON'T)

LIST OF TABLES

LIST OF FIGURES

LIST OF ACRONYMS

- NELL-1- Nel-like protein-1
- MSC- Mesenchymal stem cells
- BMP2- Bone Morphogenic Protein 2
- hPSCs- Human Perivascular Stem Cells
- BMD- Bone mineral density
- MicroCT- Micro-Computed Tomography
- ROI- Regions of interest
- SVF: Stromal vascular fraction
- ASC: Adipose-derived stem cells
- BMSC: Bone marrow-derived stem cells
- FACS: Fluorescence-activated cell sorting

Acknowledgement

This work was supported by the CIRM Early Translational II Research Award TR2-01821, NIAMS R01 AR061399-01A1 and AR066782-01.

I would like to thank my PI Dr. Kang Ting for giving me the opportunity to work on a novel exemplary project and directing me throughout this journey with his knowledge and expertise. I would also like to thank Dr. Xinli Zhang for his mentorship, teaching me new concepts and his commitment to the project. I would like to thank Soonchul Lee, Jia Shen, Aaron W. James, Chenshuang Li, Yulong Zhang, Reef Hardy, Benjamin M. Wu, Bruno Peault, David Stoker, Huiming Wang, Choon G. Chung for their collaboration, dedication and willingness to help in this study including surgery, preparation of implants, and histology.

1. Introduction

Osteoporosis is a common skeletal disease characterized by low bone mineral density (BMD) and micro-architectural deterioration of bone tissue. There are degenerative changes that accompanies osteoporosis in the intervertebral discs and spinal facet joint capsules in people over 50 years of age resulting in spinal instability and the ultimate outcome of fragility fractures. Because osteoporosis is strongly associated with poor fusion rate and bone stability, it is crucial to understand the pathophysiology of osteoporosis and its treatment, in order to enhance spinal fusion and preserve bone stability.

1.1 Pathogenesis of Postmenopausal Osteoporosis

Bone is comprised of a collection of dynamic tissues. Bone remodeling which is a process of controlled bone resorption and formation occurs in the bone microcracks continuously [14, 16]. It's carried out by basic multicellular unit (BMU) within the bone remodeling cavity, and the BMU is composed of osteoclasts, osteoblasts, bone lining cells and osteocytes [20]. Complete regeneration of adult skeleton takes 10 years through remodeling to repair damage and prevent aging and fracture [14]. Disruption of the remodeling process with increased osteoclastic activity results in reduced bone mineral density (BMD) and osteoporosis. Among several etiologies of osteoporosis, menopause is considered the most common one. Bone loss both in men and women commence in the 40's and accelerated bone loss occurs in women during 1^{st}-10^{th} year after menopause. Therefore, the incidence of fracture is higher in women than men [18].

Loss of estrogen in menopause has several effects on bone biology. Molecular changes occur which involves increased secretion of IL-1, IL-6, macrophage colony stimulating factor and TNF. These cytokines stimulate osteoclast development. Moreover, loss of the inhibitory effects of Osteoprotegerin, which is stimulated by estrogen, on osteoclastogenesis come about.

Osteoprotegerin acts by blocking the receptor activation of nuclear factor-kB (RANK)ligand/RANK interaction-- the main stimulator of osteoclast differentiation and activation. Nonetheless, cellular changes in menopause favors increased osteoclast formation which tends to persists with decreased initial mesenchymal differentiation towards osteoblasts. Estrogen deficiency leads to shorter osteoblast and osteocytes life span, and prolongation of osteoclast lifespan [17, 19]. These events will impair osteocyte-canalicular mechanoreceptors which act as skeletal signals for detection of micro-damage and repair with eventual bone loss as a downstream consequence to these changes.

1.2 Osteoporosis and Fragility, definition and prevalence

Today osteoporosis is defined as loss of bone mass and micro architectural deterioration of the bone tissue with subsequent bone fragility and increased fracture risk [1]. The World Health Organization, WHO, published an operational definition of osteoporosis: a BMD value of -2.5 standard deviations (SD) or lower compared to young adults measured with DXA technique [2]. The risk of sustaining a fragility fracture approximately doubles with each SD reduction in the BMD score, 2.6 times the risk for fracture of the femoral neck and 2.3 times for vertebral fracture [3, 4]. Vertebral fractures are a common cause of morbidity with a prevalence of 15-20% in postmenopausal women and often associated with significant prolonged pain [23, 24]. Worldwide it is estimated that one in three women and one in five men that will suffer a fragility fracture after the age of 50 years [25]. Alongside the suffering of the fracture patient, osteoporosis and subsequent fractures are a major burden to healthcare costs worldwide [26] with at least 250,000 spinal fusion surgeries performed in the United States each year [52].

1.3 Age-Related marrow adipogenesis and healing capacity in osteoporosis

Age-related increase in adipogenesis in the bone marrow further leads to decreased osteoblastogenesis [36, 38] as osteoblasts and adipocytes are derived from the same BMSCs. Subsequently, there is a natural decline in the number of osteoblasts due to aging, and literature has shown a decrease in their function and survival as well [37]. For these reasons, the biologic response to even the commonly used bone substitutes are suboptimal in such patients, in terms of efficacy and efficiency of bone regeneration and the frequency and magnitude of unwanted side effects [13]. As one of the many complications of osteoporosis is a compromised biomechanical integrity of the spine leading to limited motion and weight bearing function of the spine. Often such bone degeneration results in compression of the nerve roots, or even the spinal cord. The goal of spinal fusion surgery is to support the spine, prevent progression of deformity, and alleviate or eliminate pain. In elderly patients, iatrogenic cause of instability following spinal surgery may occur because of pre-existing degenerative changes in the facet joints and intervertebral disc. Moreover, achieving secure spinal fusion in osteoporotic patients with alternative therapies remains difficult due to reduced stem cell function and increased adipogenesis. In elderly osteoporotic patients, non-union occurred in 5 to 35% of patients who underwent spinal fusion [8, 11]. For these reasons a thorough understanding the spinal fusion biology is crucial.

1.4 Spinal Fusion Biology

Clinically relevant lumbar fusion animal models in previous literature provided information on the methods that facilitated fusion. Non-decortication of the transverse process did not result in arthrodesis as the primary vascular supply to the fusion mass originated from the decorticated bone, and not from the adjacent muscle [9, 21]. Following spinal fusion surgeries and insertion of the graft material, intramembranous bone formation occurred in the area adjacent to

the transverse processes while endochondral bone formation occurs centrally at the interface between the upper and lower halves of the bridging bone [39]. Cartilage formed from endochondral ossification has poor vascular supply and low oxygen saturation. In mid- and late stages of bone formation, bone extends towards the central zone with disappearance of cartilage [9, 10, 21]. The transient cartilageous area may explain lack of union that is found in central zones of a fusion mass [40]. Considering previously stated factors for a successful fusion, osteoinductive materials, osteoconductive scaffold and osteogenic cells are needed.

1.5 Spinal Fusion graft materials and Pharmacotherapeutic strategies

As bone formation is a coupled process between osteoblasts and osteoclasts maintaining homeostasis within bone, resorptive agents that induce osteoclasts apoptosis might not be effective in spinal fusion surgeries which necessitates new bone formation. Subsequently, the gold standard for spinal fusion surgeries is harvesting autologous cortical and cancellous bone from the iliac crest due to the presence of the three fundamental properties for a successful fusion (osteogenicity, osteoconductivity, and osteoinductivity) with eventual bonding of the graft material to the host bone (osteointegration). Osteoprogenitor cells living in the donor graft may survive during implantation with potential proliferation and differentiation to osteoblasts and eventually osteocytes. These cells represent the "osteogenic" potential of the graft [75,76]. "Osteoinduction" of the graft material, on the other hand, is the ability to stimulate and activate the host mesenchymal stem cells from surrounding tissue to differentiate into osteoblasts. This process is mediated by a cascade of signals and activations of several extra- and intracellular receptors, most importantly related to TGF-beta super-family [75, 76]. Any graft material which can serve as a scaffold for the ingrowth of new bone and facilitation of vasculogenesis with orientation of the blood-vessels into

a new Haversian system, provide an "osteoconduction" capability to the graft [74, 76], which can also be considered as graft extenders (carriers).

Although autografts have the 3 essential features for a successful grafting material, these grafts are limited in quantity and include donor-site morbidity [45, 46-48]. Therefore, other several methods of bone reconstruction and regeneration were developed namely using allograft, demineralized bone matrix (DBX), hydroxyapatite calcium phosphate (CP, TCP), autologous bone marrow aspirates, bone morphogenic proteins (BMPs), and several other related growth factors (VEGF, PDGF, etc.). However, all these other forms of bone grafts have disadvantages when compared to autologous bone graft and as such their suboptimal use [79]. For example, when bone marrow mesenchymal cells (BMSCs) have been studied for skeletal engineering applications, results showed that BMSCs have limitations, including limited autogenous supply of bone marrow aspirate, and relatively lower cell yield of BMSCs with increased risk of immunogenicity, genetic instability, and infection in in-vitro cell culture [49-51, 72-73]. CP and β-TCP have a little osteoconduction potential and thus used more as bone extenders (carriers) to be combined with other osteoinductive and osteogenic molecules [77,78].

1.6 Human Perivascular Stem Cell: A purified population with multilineage differentiation potential of MSC

Culture expandability, self-renewal and differentiation properties of stem cells are essential for their use in gene therapy and tissue-engineering applications. Mesenchymal stem cells (MSCs) are pluripotent stem cells obtained by aspiration of 10-40ml of bone marrow from the iliac crest or during bone marrow biopsy and isolated based on their adherence properties. Bone marrow-derived MSCs (BMSCs) have been used experimentally in tissue-engineering applications due to their ability for ex-vivo expansion resulting in hundreds of millions of cells

within few passages [80]. However, BMSCs have been reported to require selective sera and other growth factors for their expansion [81]. Also, patients' morbidity proposes a limitation while procuring BMSCs. Aspirating volumes larger than a few milliliters may be painful and frequently requires general or spinal anesthesia and may yield low numbers of MSCs upon processing [82]. And as samples are highly expanded, these procured BMSCs appeared to lose their differentiation and self-renewal capacity and approach senescence and/or express apoptotic features [83, 84]. This process is further complicated in osteoporotic patients due to increased adipogenesis. Although aging has negative effects on the number of osteoblasts, it has a positive effect on the number of adipogenesis and the formation of fatty marrow.

In attempt to circumvent the limitations of BMSCs, research has been directed to find alternative sources to MSCs. Literature has shown adipose tissue as a promising source of MSCs. Adipose tissue is highly accessible and abundant. The cell pellet obtained after processing of the liposapirate is called stromal vascular fraction (SVF). Adipose-derived stem cells (ASCs) was found to be at least three folds higher than BMSCs based on colony-forming unit adherent cells which comprised 3% of the SVF population [85,86]. A single milliliter of liposuction tissue aspirate can generate one-quarter a million ASCs through a single passage with an expansion of 64-fold with a 26-day period [85]. Although SVF provided significantly higher mesenchymal stem cells number and quality with less surgical risks. The SVF is well recognized to be a heterogenous population including non-stem cells, such as inflammatory, hematopoietic, and endothelial cells, which results in unreliable bone formation [49-51, 73]. With these drawbacks of currently available sources of MSC, there exists a clinical need for reliable MSC source with proven safety, purity, identity, and efficacy.

Our laboratory has identified and isolated perivascular stem cells (PSC) from adipose tissue using a fluorescence-activated cell sorting (FACS) method [27-30]. PSC are identified by their cell surface markers and include pericytes from microvessels and capillaries (which are CD34-, CD146+, CD45-), and adventitial cells from larger arteries and veins (which are CD34+, CD146-, CD45-) [33]. PSC exhibit the characteristic surface markers and clonal multilineage differentiation potential of MSC [27-30]. The evidence supporting the use of human perivascular stem cells (hPSC) for bone tissue engineering is based on our previous studies; including pancreas- and other organ-derived human pericytes resulted in robust *in vitro* osteogenic differentiation and intramuscular bone formation and angiogenesis [66]; adipose-derived hPSC form significantly increased intramuscular bone compared to patient-matched unpurified cells and demonstrate *in vivo* trophic and angiogenic effects [43,87]; as well as exhibited osteoprogenitor [34] and chondroprogenitor [35] cell types. This was accompanied by increased expression of bone morphogenic protein 2 (BMP2), BMP7, and vascular endothelial growth factor (VEGF), and resulted in robust bone formation in spinal fusion procedures on non-osteoporotic rats [44]; and lastly adipose-derived hPSC exhibited improved calvarial bone defect healing as compared to unsorted SVF [88].

1.7 NELL-1 Anti-osteoporotic, and Pro-osteogenic Properties:

Nel-like protein-1 (NELL-1) has been found to induce osseous healing in small and large animal models including osteoporotic rat models without harmful side effects [41, 42]. Interestingly, we observed an additive effect of NELL-1 and human perivascular stem cells (hPSCs) in an ectopic bone formation model [27, 43]. The purpose of this study is to determine the efficacy of hPSCs combined with NELL-1 for enhancing spinal fusion in osteoporotic rats with the goal of ultimately developing an effective and safe therapeutic method using hPSCs and NELL-1 to treat patients with osteoporosis.

2. Materials and Methods

2.1 Isolation of hPSCs

With the exception of one sample from autopsy, lipoaspirate was obtained from patients with and without osteoporosis undergoing liposuction under IRB exemption (**Table 1**). The hPSCs consisting of two populations: pericytes (CD146+, CD34-, CD45-) and adventitial cells (CD34+, CD146-, CD45-) were purified as previously described [33]. The lipoaspirate was stored at 4°C before processing and processed within 48 h of collection. The human stromal vascular fraction (hSVF) was obtained by collagenase digestion as previously described [33]. Briefly, an equal volume of phosphate buffered saline (PBS) was added to dilute the lipoaspirate. The mixture was then digested with Dulbecco's modified Eagle's medium containing 3.5% bovine serum albumin (BSA, Sigma-Aldrich) and 1mg/ml collagenase type II for 70 min under agitation at 37°C. Next, adipocytes were separated and excluded by centrifugation. The processed hSVF was suspended in red cell lysis buffer (155 mM NH_4Cl, 10 mM $KHCO_3$, and 0.1mM EDTA) and incubated for 10 min at room temperature. The incubated hSVF was re-suspended in PBS and 4', 6-diamidino-2-phenylindole (DAPI, Invitrogen) was added to exclude dead cells and filtered through a 70 μm cell filter. The resulting hSVF was immediately processed for hPSC purification. The number of live cells was calculated by trypan blue staining.

2.2 In vitro assays for osteogenesis and adipogenesis of hPSCs

The hPSCs were cultured in osteogenic or adipogenic differentiation medium containing NELL-1, or phosphate buffered saline (PBS) to compare their effects on osteogenesis and adipogenesis of hPSCs [27].

2.3 Animal model and surgical procedures

Athymic rats were used to prevent immune response to human cells. All animals were treated with postoperative medications of buprenorphine for 48 h and trimethiprim/sulfamethoxazole for 10 days, for pain management and prevention of infection, respectively. Animals were housed and experiments were performed in accordance with the guidelines of the Chancellor's Animal Research Committee for Protection of Research Subjects at the University of California, Los Angeles.

To induce osteoporosis, 41 athymic rats were ovariectomized [53]. Induction of osteoporosis was confirmed by dual energy X-ray absorptiometry 4 weeks post-OVX. Posterolateral lumbar spinal fusion was performed on n= 41, 8 week old athymic rats as previously described [54]. Rats were anesthetized using isoflurane (5% induction, 2-3% maintenance). After anesthesia induction by isoflurane inhalation, the surgical site was shaved and prepped. A posterior midline incision was made over the skin of the caudal portion of the lumbar spine. Two separate paramedian fascial incisions were made 3 mm from the midline. The transverse processes of the L4 and L5 vertebrae were exposed by blunt muscle splitting technique separating the back muscles. Subsequently, decortication of the transverse processes is carried out using a low speed electric-driven bur until a blush of cancellous bone was observed. Sterile saline irrigation has been used simultaneously during decortication to cool the decorticated site and furnish a clean surface for implantation. Next, one implant per side containing the active drug were placed between the decorticated transverse processes into the paraspinal muscle bed. Fascia and skin incisions were sutured and closed using 4-0 Vicryl absorbable sutures (Ethicon). After surgery, about 0.05 mg/kg buprenorphine was administered twice daily for 2 days postoperatively for analgesia, and 48 mg/mL

trimethoprim/sulfamethoxazole antibiotic was administered for 10 days postoperatively. All animals were sacrificed at 4 weeks by CO_2 overdose and the spines were harvested for analysis.

2.4 Implant preparation

The implants were prepared using 2 different doses of hPSCs and NELL-1 based on our previous studies: (1) Regular dose: 0.25 x 10^6 cells/ml of hPSCs or 33.3 μg/ml of NELL-1 that demonstrated the successful fusion in non-osteoporotic models [44, 54]; (2) High dose: 0.75 x 10^6 cells/ml of hPSCs or 66.6 μg/ml of NELL-1. Finally animals were organized into the following 7 implant groups: (1) Regular P: Regular dose of hPSCs alone; (2) Regular N: Regular dose of NELL-1 alone; (3) Regular P+N: Combination of regular dose of hPSCs and NELL-1; (4) High P: High dose of hPSCs alone; (5) High N: High dose of NELL-1 alone; (6) High P+N: Combination of high dose of hPSCs and NELL-1; (7) Control. A detailed discussion of each of the implant constituents is presented in **Table 2.**

2.5 Manual palpation

Manual palpation was performed to evaluate the fusion mass between the lumbar spines of rats post-harvest. The samples were palpated by three blinded observers and scored on a scale of 1 to 5 by application of flexion and extension forces manually against the L4 and L5 vertebrae as previously described [36]. The scoring criteria is summarized in **Table 3**. Scores of four or above were considered as reflective of spinal fusion.

2.6 Post-mortem high-resolution microCT evaluation

MicroCT analyses including bone volume (BV) and bone mineral density (BMD) were performed using CT-Analyzer software (SkyScan 1172, Belgium). Animals were sacrificed at 4 weeks post-treatment and harvested for lumbar vertebrae. Samples were fixed in 4% paraformaldehyde (PFA) for 48 hours and stored in 70% EtOH for microCT. Later, EDTA

(Ethylenediaminetetraacetic acid) was used for decalcification for histological, and immunohistochemical analyses. Lumbar vertebrae were scanned using a high-resolution microCT (SkyScan 1172, Bruker MicroCT N.V., Kontich, Belgium) at an image resolution of 27.4 µm (55kV and 181 mA radiation source; 0.5-mm aluminum filter). Then, 3D images were reconstructed from the 2D X-ray projections by implementing the Feldkamp algorithm, and appropriate image corrections including ring artifact correction, beam hardening correction, and fine-tuning were processed using NRecon software (SkyScan 1172, Belgium). The dynamic image range (contrast limits) was determined at 0-0.1 in units of attenuation coefficient and applied to all datasets for optimum image contrast.

After acquisition and reconstruction of datasets, images were first reoriented on each 3D plane using DataViewer software (SkyScan 1172, Belgium) to align the long axes of the lumbar vertebrae parallel to coronal and sagittal planes (**Fig.1A**). Then, 3D morphometric analyses of the L4 and L5 of lumbar vertebrae were performed using CT-Analyzer software (SkyScan 1172, Belgium). The region of interest was defined as starting from the lower border of transverse process of L5 to the upper border of the transverse process of L4. Region-of-interest (ROIs) were delineated using a freehand drawing tool while maintaining clearance from the cortical boundaries of the transverse process and vertebral body (**Fig.1B**). Only graft material and new bone formation between the transverse processes of L4 and L5 were analyzed and quantified (**Fig.1C**).

A global threshold of 60-120 was applied to all scans to obtain an accurate representation of the new bone formation between the vertebrae [55] (**Fig. 1D**). Morphometric parameters were then computed from the binarized images using direct 3D techniques (marching cubes and sphere-fitting methods), and included bone mineral density (BMD, g/cm^3), and bone volume (BV, mm^3) (**Fig. 1D**). All quantitative and structural parameters followed the nomenclature and units

recommended by the American Society for Bone and Mineral Research (ASBMR) Histomorphometry Nomenclature Committee [56]. After data quantification, 3D rendered models were generated for the visualization of analyzed regions using the marching cubes method.

2.7 Histology and immunohistochemistry on decalcified tissue

After decalcification in 19% ethylenediaminetetraacetic acid, the samples were embedded in paraffin. H&E and immunohistochemistry for bone sialoprotein (BSP) (Chemicon) were performed as previously described [57].

2.8 Bone dynamic labeling and hPSCs tracking on undecalcified tissue

To visualize bone-forming activity, the selected animals were injected with Calcein/Alizarin prior to sacrifice. Frozen sections were cut following Kawamoto's procedure [58]. Immunofluorescent staining for human-specific major histocompatibility complex (hMHC) class I antigen (Santa Cruz Biotechnology) was performed and analyzed using the Olympus image system.

2.9 Statistics

A paired *t*-test was used to test significance when only two groups were tested after normality test. Kruskal–Wallis test with post-hoc tests of Bonferroni was used to test the significance of data to compare more than two groups. The statistical software, SPSS for Windows Version 18.0 (SPSS, Chicago, IL, USA) was used for all statistical analyses. Statistical significance was determined $p<0.05$.

3. Results

3.1 Similar osteogenic capacity of hPSCs from osteoporotic and non-osteoporotic conditions

No significant difference in osteogenic differentiation was observed between the healthy and osteoporotic donors. Interestingly, the addition of NELL-1 enhanced mineralization of hPSCs

from both types of donors without significant differences (**Fig. 2**). The additional experiment under adipogenic induction revealed that, in contrast to BMP-2, hPSCs treated with NELL-1 did not undergo more adipogenic differentiation compared to PBS control ($p>0.05$), although hPSCs from osteoporotic donors displayed inherently higher adipogenic differentiation compared to its healthy counterpart (**Fig. 2**). Notably, the average yield of hPSCs from listed donors did not differ significantly from each other (**Table 1**).

3.2 hPSC+NELL-1 increased fusion rate in the osteoporotic rats

Post-OVX, the average BMD of the L5 vertebrae significantly decreased by 10.2% compared to its preoperative state ($p<0.01$) (**Fig. 3**). Among seven groups, High P+N group exhibited significantly increased palpation scores (4.7) with the highest fusion rate at 83.3% (**Fig. 4F**) compared to the other study groups ($p<0.01$) (**Fig. 4A, 4B, 4C, 4D, 4E**). Notably, neither the regular dose which was effective for healthy rats [44, 54] nor high dose of hPSCs or NELL-1 alone could produce a significant fusion rate in OVX rats (**Table 2**), with only 20% fusion rate in Regular NELL-1, regular hPSCs and high NELL-1 groups while high hPSCs fusion rate was 28.6% (**Fig. 4A, 4B, 4C, 4D**).

3.3 Robust bone formation promoted by hPSC+NELL-1 in the osteoporotic rats

Three dimensional micro-CT images showed that High P+N formed new bony masses between the transverse processes resulting in solid fusion. In contrast, the control group demonstrated clear clefts between the two transverse processes with minimal bone formation. Quantitatively, the High P+N group exhibited a significant increase in BV of 82.6 ± 1.97 mm^3 compared to any other groups ($p<0.01$) (**Fig. 5**). However, the samples with regular dose did not exhibit a significant difference (**Fig. 7**). Histologically, the fibrous tissue formation was prevalent in the control, High N and High P samples. In contrast, we observed large areas of chondroid

matrix with bone formation, increased vascularization and complete bony bridging in High P+N specimens. Additionally, BSP immunohistochemistry demonstrated increased staining in new bone and cartilaginous tissue in High P and High P+N samples compared to the control samples. (**Fig. 6A**).

3.4 Tissue engraftment revealed involvement of hPSCs in active ossification

We observed a wider band of Calcein/Alizarin labeling in High P+N than other groups, suggesting more robust active ossifications along the edges of the dimeneralized bone matrix (**Fig. 6B**). We merged the images of hMHC Class I immunofluorescent staining with Calcein/Alizarin labeling and found that hPSCs and new bone formation were co-located in the same region, confirming the direct involvement of hPSCs *in situ* of the active ossification (**Fig. 6C**).

4. Discussion

One of the most promising emerging surgical options maybe the use of "composite graft" that comprise osteogenic capacity with osteoinduction properties along with osteoconductive scaffold. Recent developments in regenerative medicine support the crucial role that stem cells play in bone regeneration. However, most studies are designed using a healthy animal to create disease models [44, 69]. In order to replicate clinical osteoporotic settings, it becomes critical to demonstrate the efficacy of these stem cell therapeutics in osteoporotic animals. To our knowledge, this is the first study that clearly demonstrated the great potential of combinatorial application of stem cells (hPSCs) and osteogenic factor (NELL-1) in promoting successful spinal fusion in osteoporotic rats.

Although not yet fully understood, delayed fusion or nonunion in osteoporotic bone have been attributed to: (1) decreased proliferation and differentiation capacity of endogenous

mesenchymal stem cells; (2) diminished formation of vasculature; (3) lower osteoinductive activity; and (4) changes in local and systemic signaling molecules [59].

In agreement with prior studies, we observed that the healing potency of osteoporotic bone was severely impaired compared to its healthy counterpart **(Table 4)** [60-64]. Only 20% of fusion was achieved in osteoporotic rats using the same number ($0.25x10^6$ cells/ml, regular dose) of hPSCs that induced 100% fusion in non-osteoporotic rats [44].

It was reported that stem cells from fat, even from osteoporotic patients, can undergo osteogenic differentiation at a similar rate to bone marrow stem cells (BMSCs) from younger patients [70]. Our study revealed similar osteogenic capacity of hPSCs from lipoaspirate between donors with and without osteoporosis. Considering the defects in osteogenic property of BMSCs from osteoporotic condition [71], these characteristics of hPSCs will be a good building block in the development of efficacious and safe therapy using autologous stem cells from adipose tissue in an orthopaedic clinical setting. The hPSCs induce bone formation via both direct osteogenic differentiation and indirect trophic effects. They secrete high levels of pro-osteogenic, pro-vasculogenic growth factors, such as vascular endothelial growth factor, fibroblast growth factor 2, and epidermal growth factor [33,43].

There are several advantages to using NELL-1 in osteoporotic conditions over BMP-2: (1) NELL-1 inhibits BMP-2 induced inflammation by acting as an anti-inflammatory molecule [67]. (2) NELL-1 has anti-osteoclastic effects [42]. (3) NELL-1 inhibits adipogenic differentiation [68]. In previous studies [65], we observed NELL-1 could stimulate proliferation of hPSCs. Consequently, we suggest that the administration of hPSCs+NELL-1 restores the reduced native osteoprogenitor cell and osteoinductive microenvironment in osteoporotic bone. In the current study, the direct

involvement of hPSCs in active ossification was further validated by a novel cryostat sectioning technique using undecalcified samples.

However, further studies with larger sample size focusing on the mode of action of this promising therapy and on any differences of osteogenic capacities of hPSCs from obese and slim donors are warranted. It is unclear if differences in body mass index translate to differences in hPSC behavior, as has been previously reported in adipose derived stem cells [66]. The synergistic effects of hPSCs and NELL-1 in enhancing spinal fusion with osteoporotic condition shed light on possibility of developing hPSCs based therapy for osteoporotic patients.

5. Conclusion

Human adipose tissue derived hPSCs from both non-osteoporotic and osteoporotic conditions exhibited similar osteogenic capacity and responsiveness to osteoinductive factor in vitro. The hPSC combined with NELL-1 synergistically enhances spinal fusion in osteoporotic rats and has great potential as a novel therapeutic strategy for osteoporotic patients.

6. Tables and Figures

Table 1. List of human lipoaspirate samples used for current study

Samples	Gender/Age	SVF yield[b]	SVF viability	Ratio of hPSCs in SVF	hPSCs yield	Average hPSCs yield[b]
OP 1	F/43	27.8×10^6	87.4%	0.49	11.9×10^6	
OP 2[a]	F/35	37.7×10^6	77.5%	0.47	13.7×10^6	$(12.4 \pm 1.1) \times 10^6$
OP 3[c]	F/71	36.0×10^6	93.0%	0.35	11.7×10^6	
Non-OP 1	F/44	28.5×10^6	87.6%	0.49	12.2×10^6	
Non-OP 2	F/25	33.2×10^6	75.9%	0.42	10.5×10^6	$(10.4 \pm 1.9) \times 10^6$ [d]
Non-OP 3	F/34	24.3×10^6	81.3%	0.42	8.4×10^6	

[a]This sample was from a patient with steroid induced osteoporosis.

[b]100 ml of pure fat tissues was used.

[c]This adipose sample (abdominal fat) was from an autopsy, not lipoaspirate.

[d]No significant difference of average hPSCs yield between non-osteoporotic and osteoporotic samples, $p>0.05$. Additionally, this number was not significantly different with average yield of hPSCs from 173 non-osteoporotic/healthy donors accumulated in our lab.

OP: osteoporosis, SVF: stromal vascular fraction, hPSCs: human perivascular stem cells.

Table 2. Composition of different implant groups and summary of the manual palpation score, fusion rate.

Group (n)[a]	Implant materials and dose (per side)				Palpation score	Fusion rate (n)
	hPSCs (cells/ml)	NELL-1 (μg/ml)	β-TCP[b](mg)	DBX (μl)		
High P + N(6)	0.75 x 10^6	66.6	50	300	4.7[c]	83.3% (5/6)
High P(7)	0.75 x 10^6	0	50	300	3.5	28.6% (2/7)
High N(5)	0	66.6	50	300	3.5	20% (1/5)
Regular P+N(8)	0.25 x 10^6	33.3	50	300	3.4	37.5% (3/8)
Regular P(5)	0.25 x 10^6	0	50	300	3.2	20% (1/5)
Regular N(5)	0	33.3	50	300	3.1	20% (1/5)
Control(5)	0	0	50	300	2.2	0% (0/5)

[a]Regular P or regular N means that number of hPSCs or concentration of NELL-1 that demonstrates the successful fusion in non-osteoporotic models [44, 54]. High P or high N means the three times higher number of hPSCs compared to regular P or two times higher concentration of NELL-1 compared to regular N in each. P+N means the combination of hPSCs and NELL-1 with regular or high dose. Control means the implant without hPSCs and NELL-1.

[b]NELL-1 carried into the DBX after lyophilization onto β-TCP.

[c]Significantly higher palpation score than any other groups.

Abbreviations: DBX, demineralized bone matrix; N: NEL-like protein-1 (NELL-1), P: human perivascular stem cells (hPSCs), SF: spinal fusion, β-TCP: beta tri-calcium phosphate particles.

Table 3. Manual palpation score

Score[a]	Description
1	Motion between vertebrae, with no bone mass formation
2	Motion with a unilateral bony mass
3	Motion with bilateral bony masses
4	No motion between vertebrae, with moderate bilateral bone masses bridging transverse processes
5	No motion, with abundant bilateral bone masses bridging transverse processes

[a]Successful fusion was determined to be a spinal column receiving an average score of 4 and above.

Table 4. Limitations of spinal fusion in osteoporotic bone: Comparing the results of spinal fusion between osteoporotic and non-osteoporotic bone

Study	Surgery	Time[a]	Group				Findings
			Model	Material	Dose[b]	Fusion	
Takahata[60]	B PLF	4 weeks	Sham	ABGs	0.2g	50%	Sham group had better histomorphometric results in the analyses of microcomputed tomography than the OVX.
			OVX	ABGs	0.2g	38%	
Nakao[61]	B PLF	8 weeks	Sham	ABGs	0.3g	91%	The number of osteoclasts in the OVX group was significantly more than in the sham group.
			OVX	ABGs	0.3g	77%	
Moazzaz[62]	B PLF	3 weeks	Sham	BMP-7	15µg	100%	Bone formation was present in non-OVX rats with bilateral fusion masses, but OVX rats did not demonstrate evidence of new bone formation.
			OVX	BMP-7	15µg	0%	
Lu[63]	B PLF	3 weeks	OVX	BMP-7	15µg	0%	Bone formation in osteoporotic rats is delayed in comparison to rats without osteoporosis and required a 3x higher dose of BMP-7 to achieve bone formation.
			OVX	BMP-7	45µg	85%	
Park[64]	B PLF	4 weeks	Sham	ABGs	0.25g	70%	The Sham group showed increased fibrous, cartilage, trabeculation ratio and bone remodeling, but the OVX group showed the opposite pattern.
			OVX	ABGs	0.25g	30%	

[a]The time interval between spinal fusion and the harvest.

[b]Dose of material per implant.

B: Bilateral, U: Unilateral, PLF: Posterolateral fusion, OVX: Ovariectomy, ABG: Autologous bone grafts, BMP: Bone morphogenetic protein.

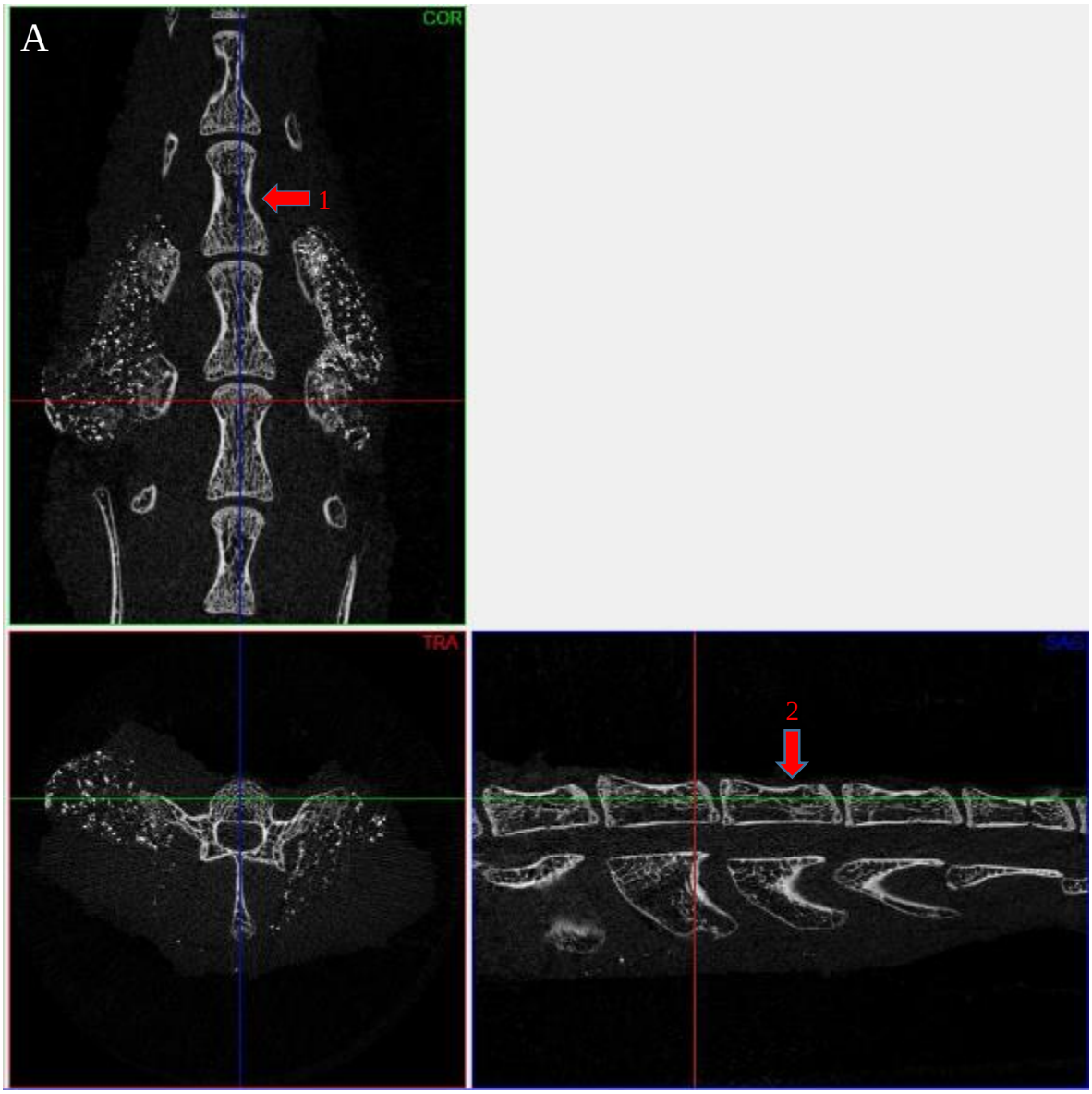

Figure 1A. MicroCT DataViewer software for sample alignment in all 3 planes- coronal, sagittal and transverse. The figure shows the sample aligned parallel to the coronal (arrow1) and sagittal (arrow2) sections before being analyzed and quantified.

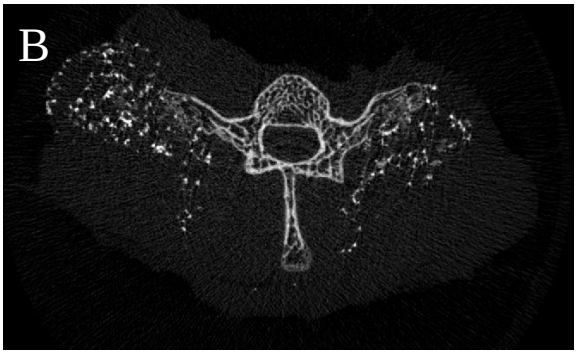

Figure 1B. Original sample cut of the microCT.

Figure 1C. Region-of-Interest (ROI) on the CTAn software of the SkyScan microCT machine. Freehand drawing tool was used while maintaining clearance from the cortical boundaries of the transverse process and vertebral body.

Figure 1D. Only new bone formation between the transverse processes of L4 and L5 were analyzed and quantified. The threshold for quantification of the graft material along with the new bone formation was set between 60-120 to exclude all the β-TCP graft material while quantifying only new bone. In this case, only the greyscale density of only the pixels that are binarised to white are quantified.

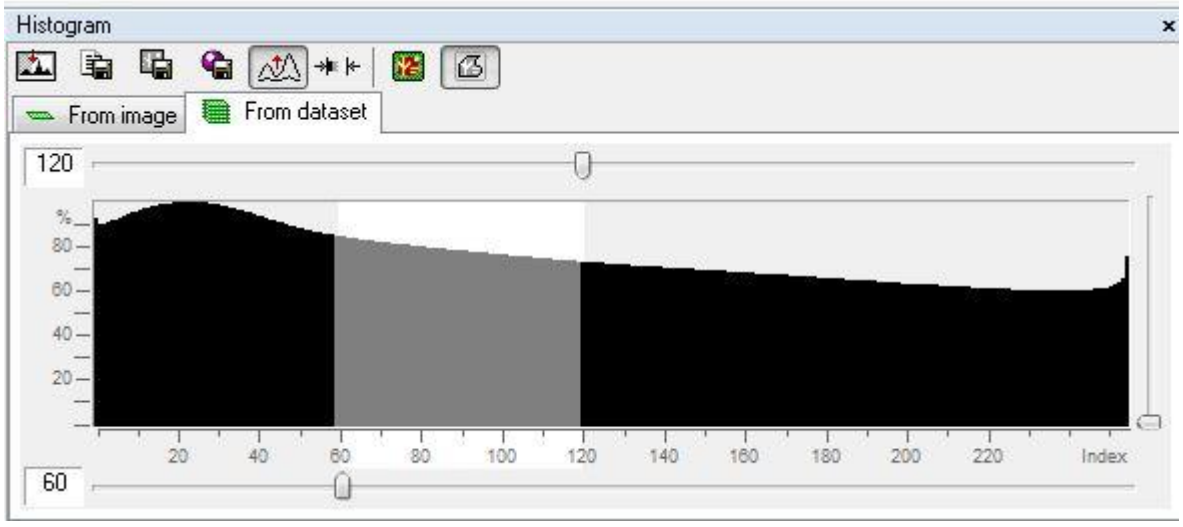

Figure 1E. Calibrated BMD for new bone formation excluding graft material using the binary threshold.

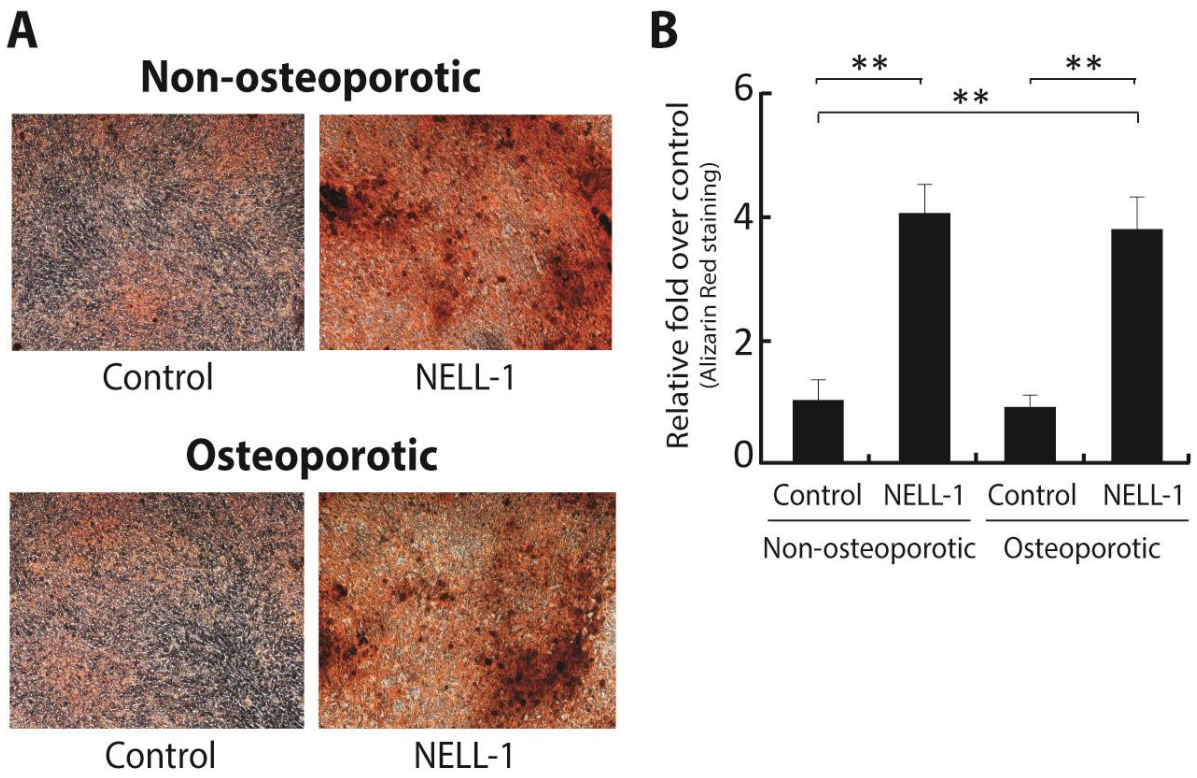

Figure 2. Adipose tissue derived hPSCs retain their osteogenic potential and NELL-1 responsiveness with osteoporosis. The hPSCs underwent osteogenic differentiation over a time period of 15 days. Cells were seeded at $3x10^4$ density, in 24 well plates with Dulbecco's modified Eagle's medium (DMEM) +10% fetal bovine serum (FBS). Within 24 hours, cells were induced to osteogenic differentiation by NELL-1 (300 ng/ml) or phosphate buffered saline control in osteogenic differentiation medium (DMEM+10% FBS+50 mg/ml ascorbic acid, and 10 mM β-glycerophosphate). Media was changed every 3 days. (A): Osteogenic differentiation was determined by Alizarin Red staining. (B): Quantification of osteogenesis of hPSCs derived from non-osteoporotic and osteoporotic patients showed that osteogenesis was significantly increased in both groups when the hPSCs were cultured with NELL-1, and there were no significant differences on basal and NELL-1-induced osteogenic properties between hPSCs from non-osteoporotic and osteoporotic patients. **, $p<.01$ compared to the control-treated hPSCs. Bars ±SD. Abbreviation: NELL-1: Nel-like protein-1.

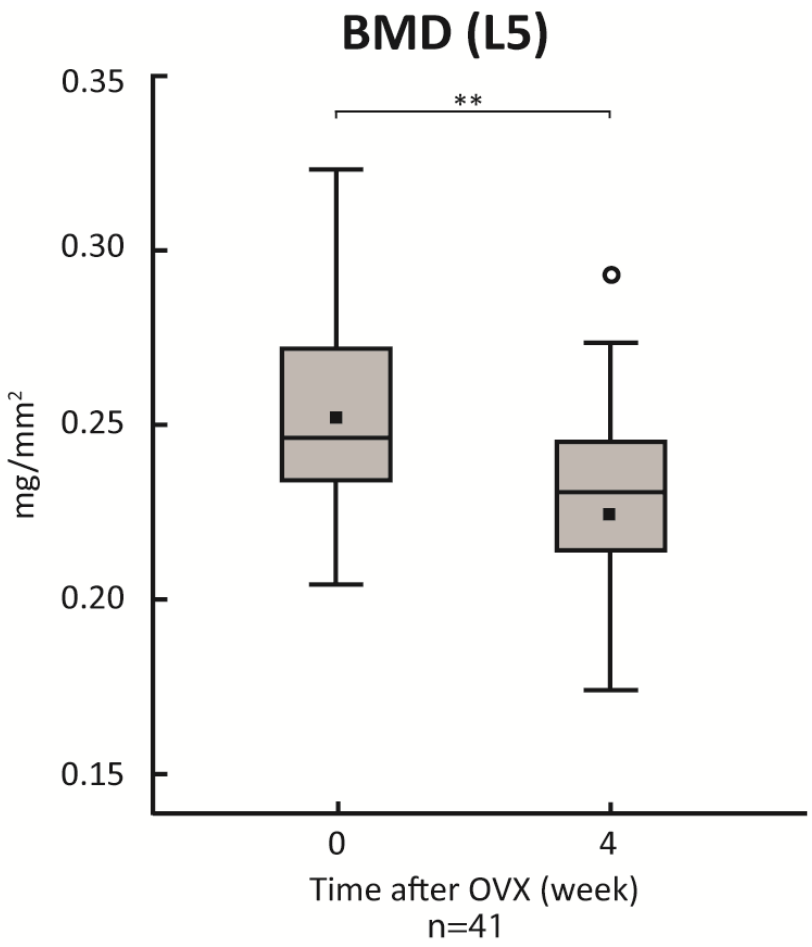

Figure 3. Confirmation of rat osteoporotic condition after OVX. The BMD of L5 measured by DEXA was used to verify the successful induction of osteoporosis 4 weeks post-OVX using Lunar PIXImus 2 2.0 software (Lunar PIXImus, Madison, WI, USA), with absolute BMD values expressed in milligrams per square millimeter (mg/mm^2). The BMD of L5 decreased significantly 4 weeks after OVX. Black square: mean value of each time point, BMD: bone mineral density, OVX: ovariectomy, DEXA: dual energy X-ray absorptiometry, ** $p<0.01$.

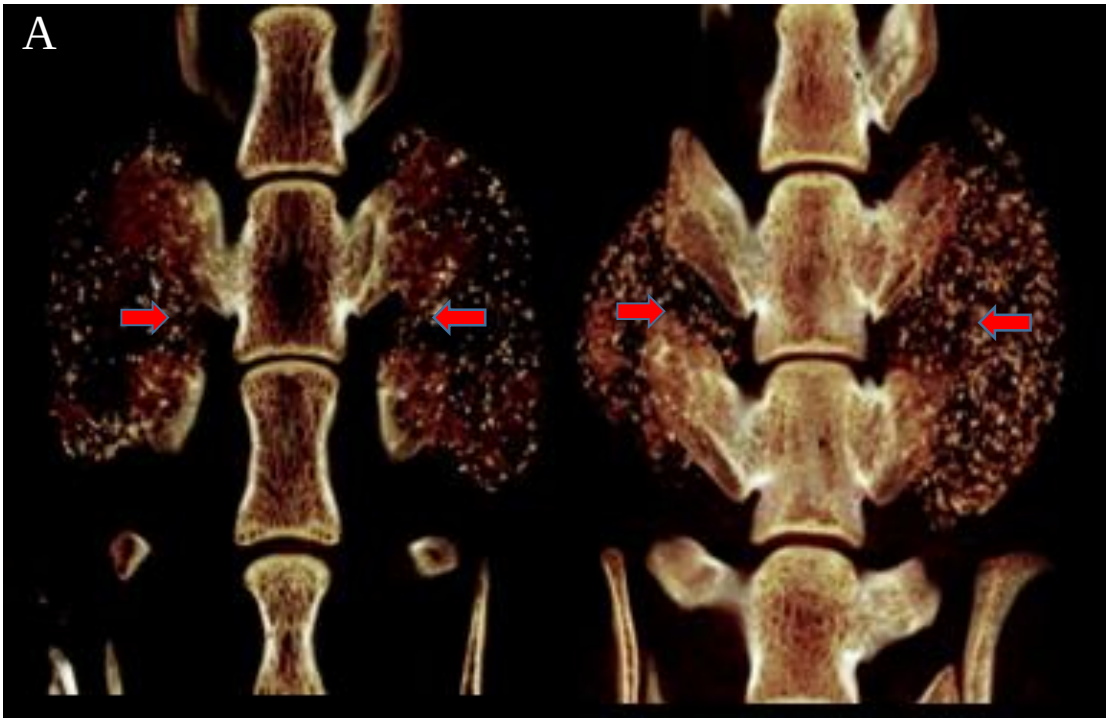

Fig.4A. Regular NELL-1 representative samples with fusion rate 20% by manual palpation.

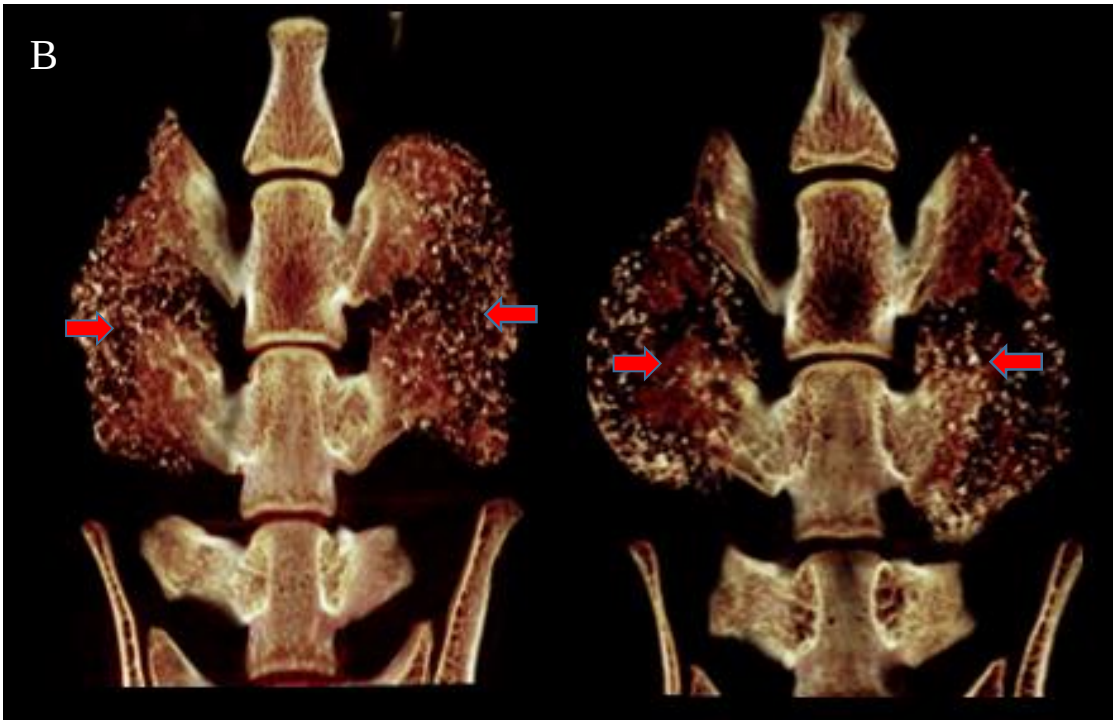

Fig. 4B. High NELL-1 representative samples with fusion rate 20% by manual palpation.

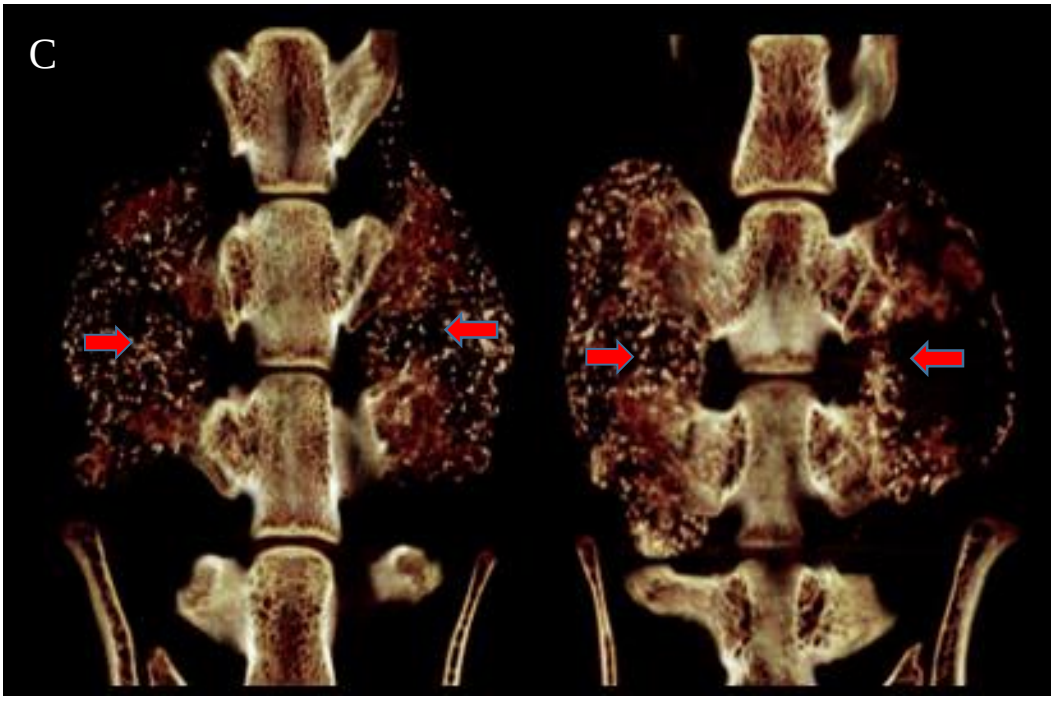

Fig. 4C. Regular hPSCs representative samples with fusion rate 20% by manual palpation.

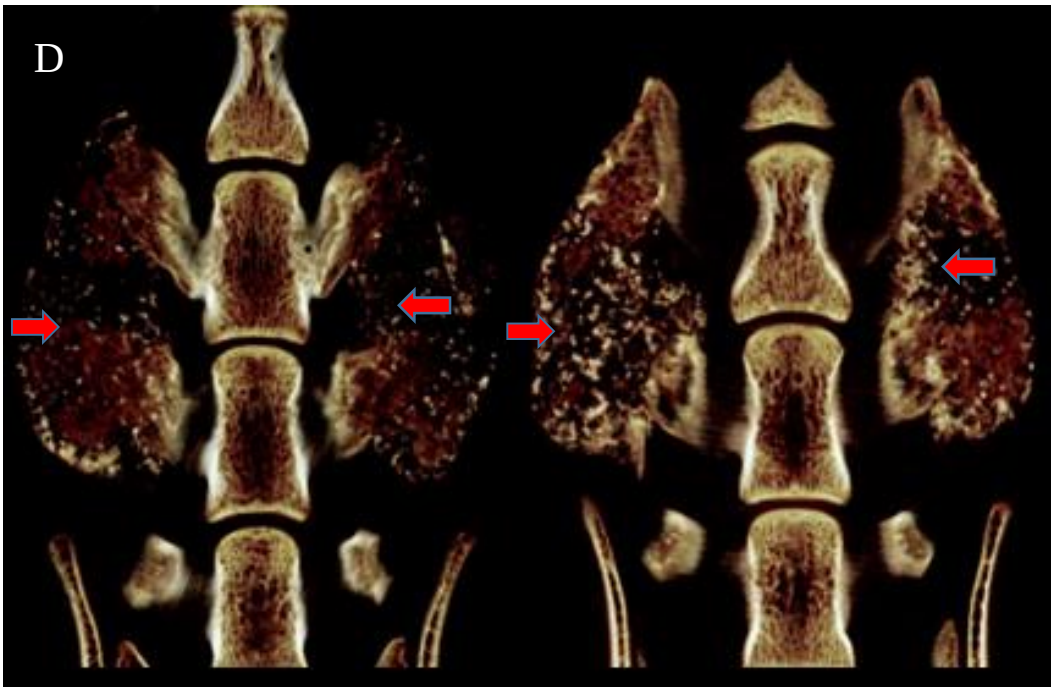

Fig. 4D. High hPSCs representative samples with fusion rate 28% by manual palpation.

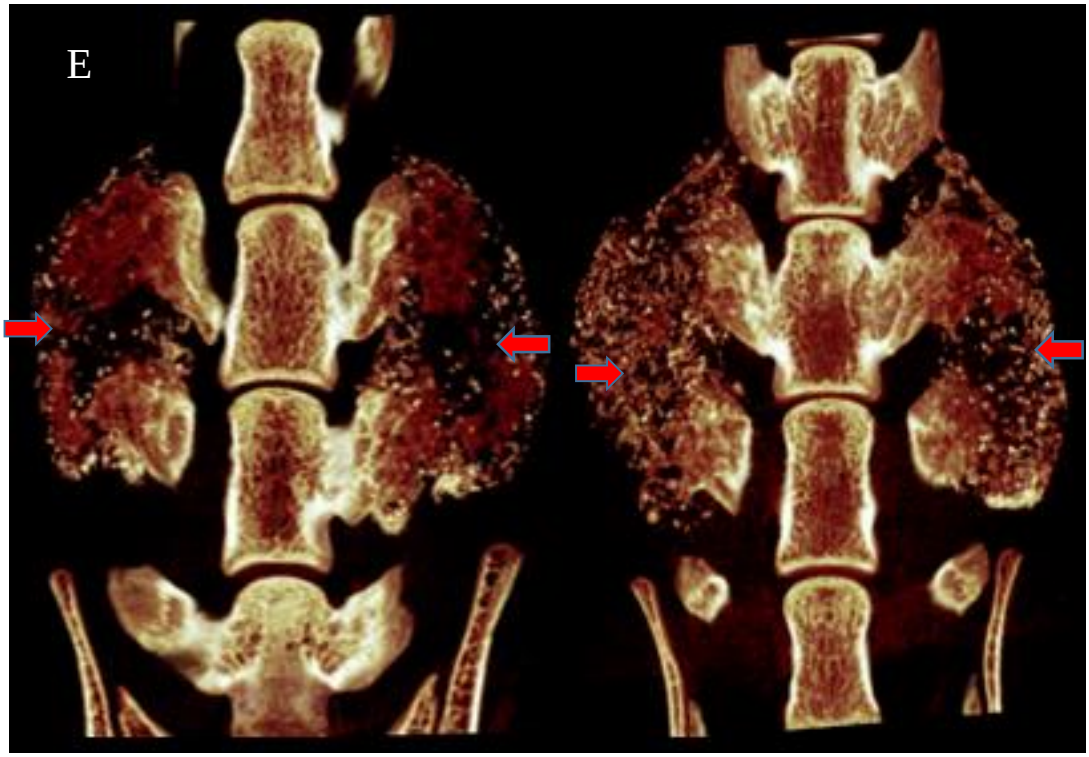

Fig. 4E. Regular hPSCs+ NELL-1 representative samples with fusion rate 37.5% by manual palpation.

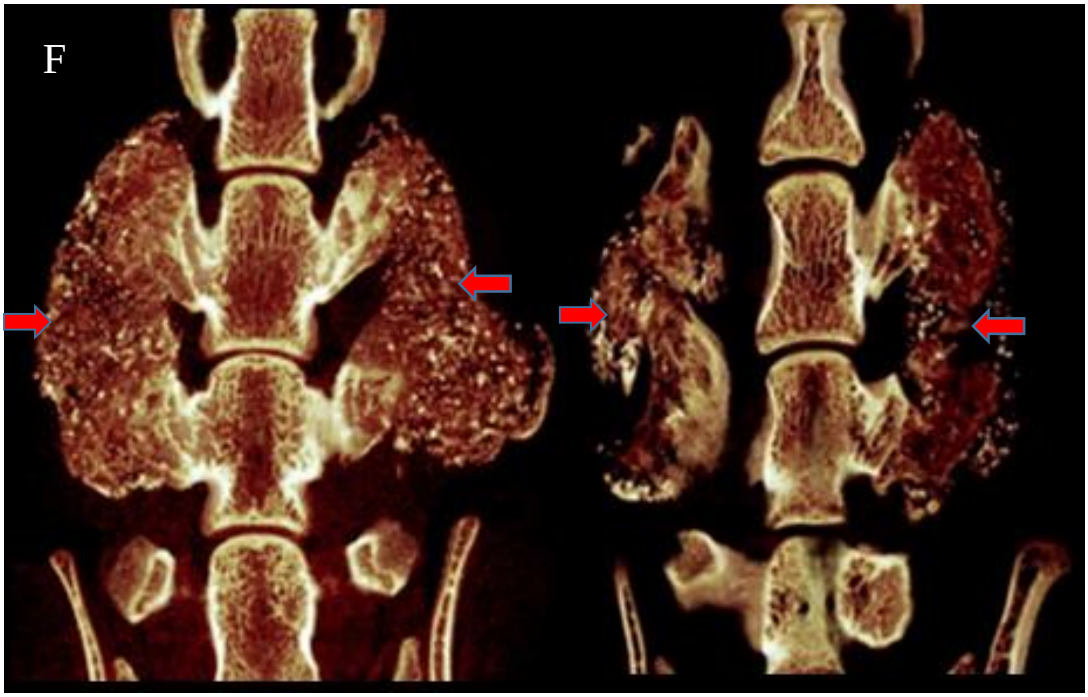

Fig. 4F. High hPSCs+ NELL-1 representative samples with fusion rate 83.3% by manual palpation.

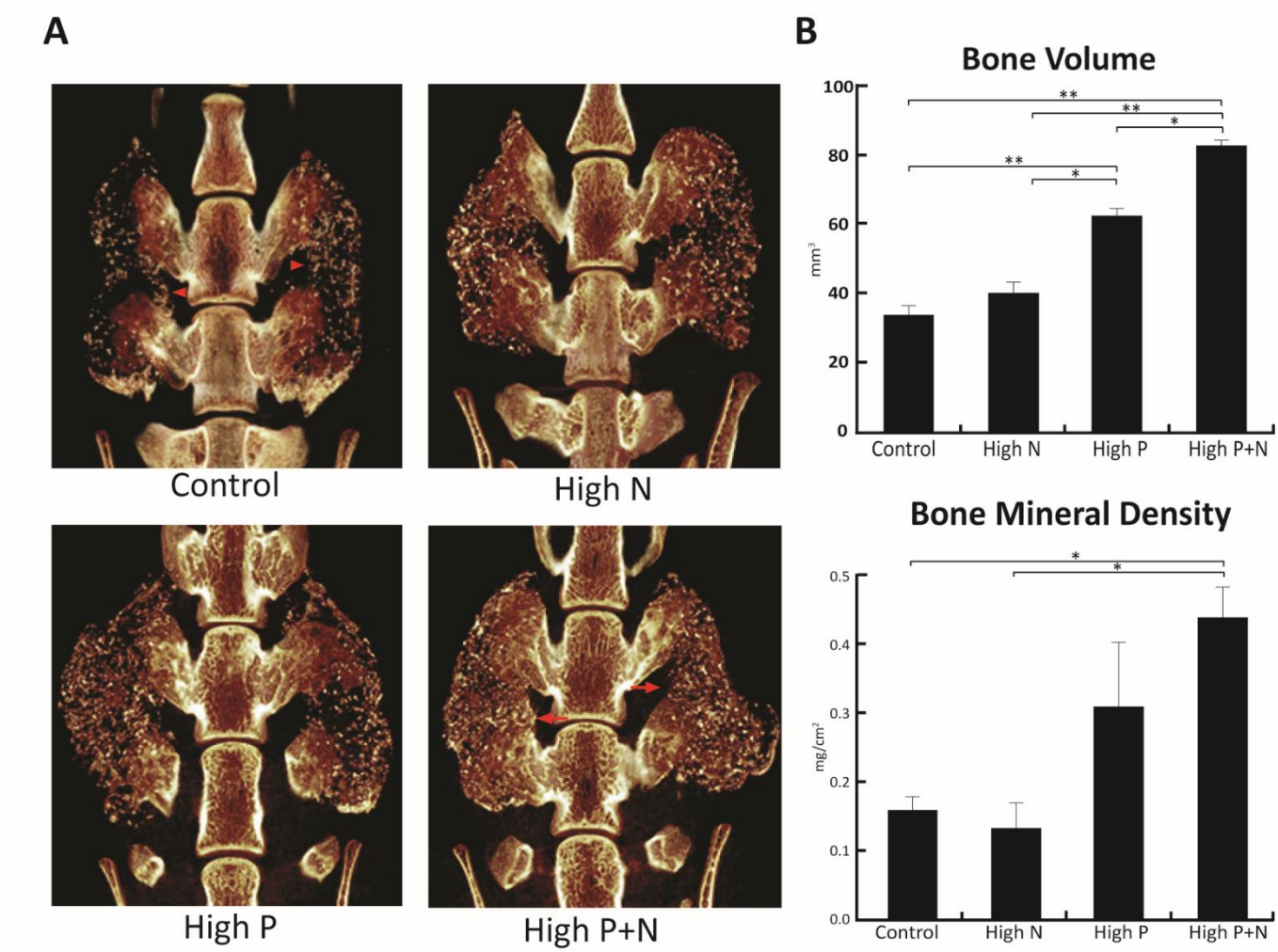

Figure 5. hPSCs +NELL-1 promotes solid bony fusion in osteoporotic rat. (A): Representative images of microcomputed tomography scanning of fusion mass with three-dimensional reconstruction from high P+N, high P, high N, and control groups 4 weeks after implantation. The high P+N group had marked bone formation around the transverse processes of L4 and L5 (arrow). In contrast, the control group demonstrated radiolucent spaces (arrow head).

(B): Histomorphometric analyses of the fusion mass showed a significant increase in bone volume in rats treated with high P+N. The region of interest was defined as starting from the lower border of transverse process of L5 to the upper border of the transverse process of L4. Only graft material and new bone formation between the transverse processes of L4 and L5 were analyzed and quantified. *, p<.05; **, p<.01. Bars±SD. Abbreviations: N, Nel-like protein-1; P, human perivascular stem cells.

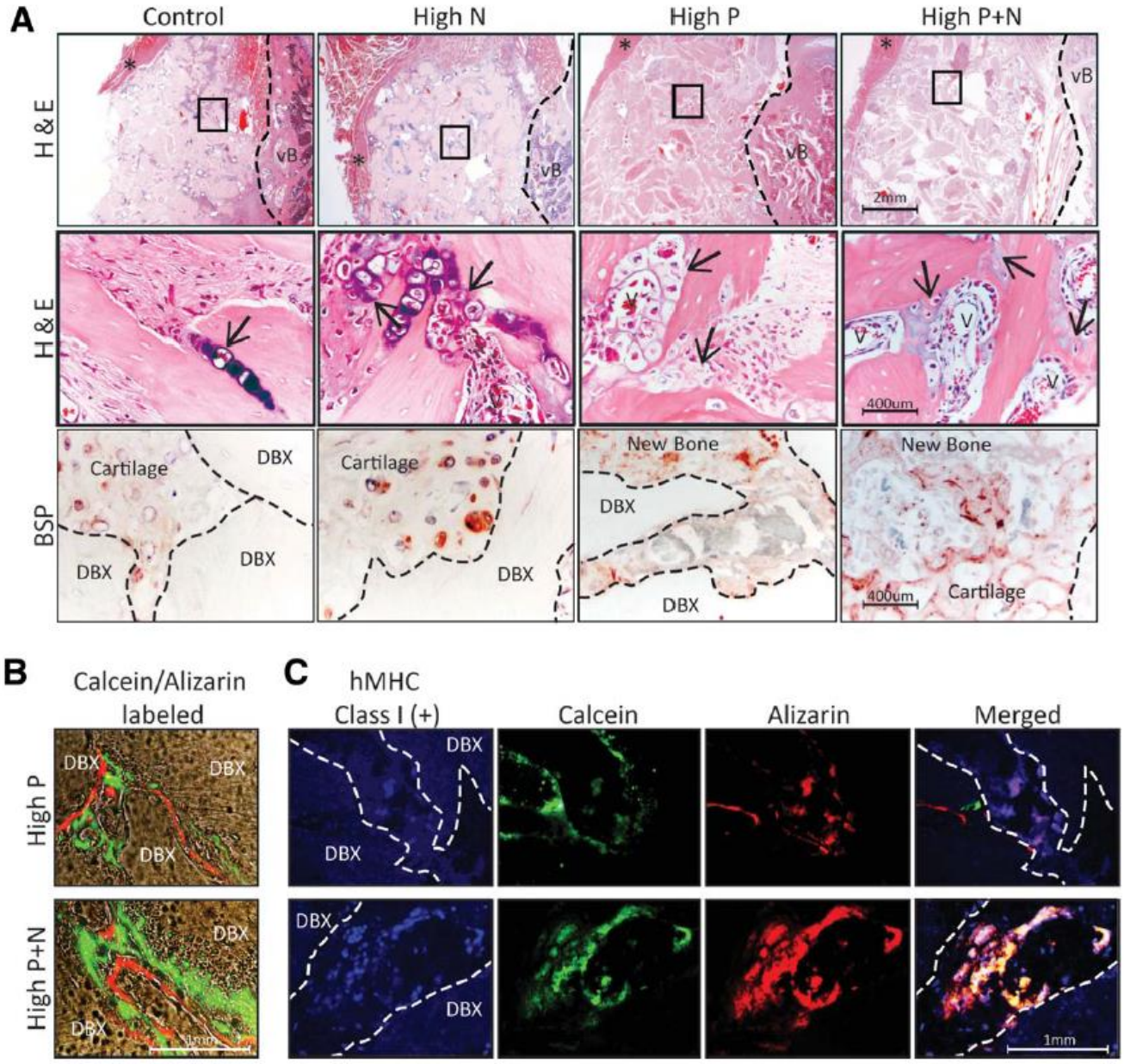

Figure 6. Histologic evidence of new bone formation and direct involvement of hPSCs in active ossification. (A): Top panel: H&E staining in low magnification images showing a dash line divides the bone mass formed over the transverse processes of vertebral bones (vB). The asterisk indicates the capsule of bone mass over the transverse processes. Middle panel: H&E staining in

high magnification of black box area of corresponding top panel image reveals more active and mature bone formation areas (arrows) and blood vessels (V) in high P+N group over either high P or high N. Bottom panel: Immunohistochemical staining demonstrated positive brown staining for the BSP. In control and high N groups, the BSP positive chondrocytes were shown without bone formation. New bone and cartilage tissues were stained BSP positive in high P and high P+N samples. Overall, more positive cells were revealed in high P+N samples. (B): The active ossifications were observed along the edge of DBX particles (dark gray) using Calcein (green) and Alizarin complexone (red) dynamic labeling in the superimposed images of bright light and fluorescent fields. Samples from high P+N revealed more robust activity of new bone formation in cryosection of undecalcified tissue. (C): The hMHC class I positive hPSCs were colocalized/embedded in mineralized matrix in cryosection of undecalcified tissue. Higher numbers of hPSCs positive of MHC class I (blue) were observed in high P+N group compared to high P. When the images were merged, bone formation was specifically correlated with the area of hPSCs (pink). Images were acquired at 340 magnification for the top panel of (A) and 3200 magnification for middle and bottom panel of (A) and (B, C) originally, and the relevant scale bars were provided. Abbreviations: BSP, bone sialoprotein; DBX, demineralized bone matrix; H&E, hematoxylin and eosin; hMHC, human major histocompatibility complex; hPSCs, blue by Aminomethylcoumarin streptavidin or pink by merging with green and red; N, Nel-like protein-1 (NELL-1); P, human perivascular stem cells (hPSCs).

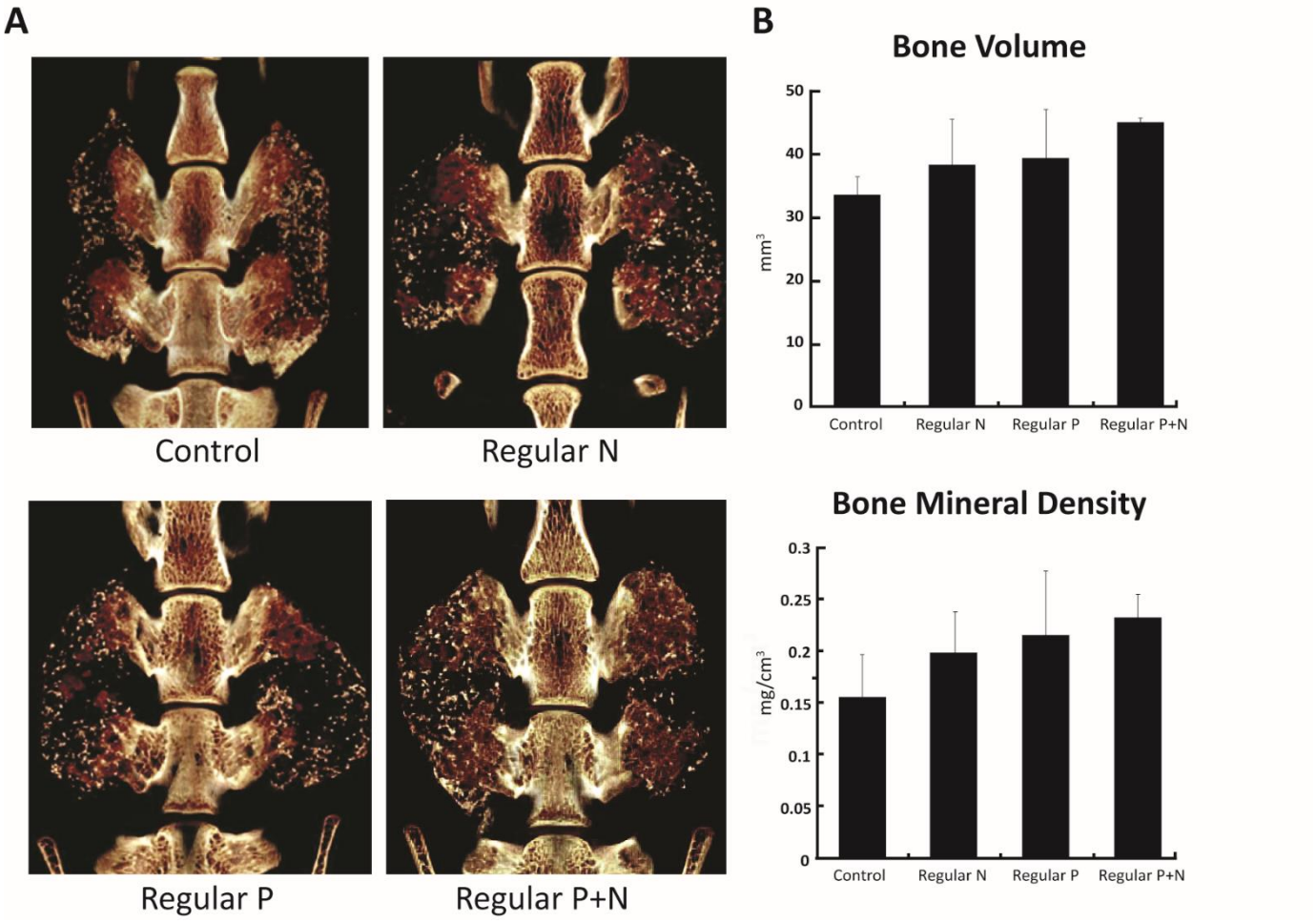

Figure 7. MicroCT of spinal fusion in OVX rats with regular dose of hPSCs and/or NELL-1. (A) Representative images of microCT 3 dimensional reconstruction from Regular P+N, Regular P, Regular N, and control groups. All of the regular dose samples showed only scant bone around the transverse processes of L4 and L5 similar to the controls, which means that the regular dose of implant materials does not work in osteoporotic bone. (B) Quantitatively, there was no significance difference in BV and BMD among the regular dose groups and control. MicroCT: micro-computed tomography, P: human perivascular stem cells (hPSCs), N: *Nel*-like protein-1 (NELL-1), BV: bone volume, BMD: bone mineral density. Bars, ±SD

REFERENCES

1. Consensus development conference: prophylaxis and treatment of osteoporosis. Osteoporos Int, 1991. 1(2): p. 114-7.

2. Kanis, J.A., Assessment of fracture risk and its application to screening for postmenopausal osteoporosis: synopsis of a WHO report. WHO Study Group. Osteoporos Int, 1994. 4(6): p. 368-81.

3. Phillips, P.J. and G. Phillipov, Bone mineral density - frequently asked questions. Aust Fam Physician, 2006. **35**(5): p. 341-4.

4. Marshall, D., O. Johnell, and H. Wedel, Meta-analysis of how well measures of bone mineral density predict occurrence of osteoporotic fractures. BMJ, 1996. 312(7041): p. 1254-9.

5. Montagnani A, Gonnelli S, Alessandri M, Nuti R. Osteoporosis and risk of fracture in patients with diabetes: an update. Aging Clin Exp Res.23:84-90. 2011.

6. Kassem M, Marie PJ. Senescence-associated intrinsic mechanisms of osteoblast dysfunctions. Aging Cell.10:191-7. 2011.

7. Giannoudis P, Tzioupis C, Almalki T, Buckley R. Fracture healing in osteoporotic fractures: is it really different? A basic science perspective. Injury.38 Suppl 1:S90-9. 2007.

8. Boden SD: Overview of the biology of lumbar spine fusion and principles for selecting a bone graft substitute. Spine (Phila Pa 1976) 15: S26- S31, 2002.

9. Boden SD: The biology of posterolateral lumbar spinal fusion. Orthop Clin North Am 29: 603-619, 1998.

10. Boden SD, Schimandle JH, Hutton WC, Chen MI: The use of an osteoinductive growth factor for lumbar spinal fusion. Part I: Biology of spine fusion. Spine (Phila Pa 1976) 20: 2626-2632, 1995.

11. Bridwell KH, Sedgewick TA, O'Brien MF, Lenke LG, Baldus C : The role of fusion and instrumentation in the treatment of degenerative spondylolisthesis with spinal stenosis. J Spinal Disord 6: 461-472, 1993.

12. Dominguez LJ, Di Bella G, Belvedere M, Barbagallo M. Physiology of the aging bone and mechanisms of action of bisphosphonates. Biogerontology.12:397-408.

13. Khan SN, Lane JM. The use of recombinant human bone morphogenetic protein-2 (rhBMP-2) in orthopaedic applications. Expert Opin Biol Ther.4:741-8. 2004.

14. Khosla S, Westendorf JJ, Oursler MJ: Building bone to reverse osteoporosis and repair fracture. J Clin Invest 118: 421-428, 2008.

15. Lindsay R: Sex steroids in the pathogenesis and prevention of osteoporosis in Riggs BL (ed): Osteoporosis: Etiology, Diagnosis and Management. New York: Raven Press, 1988, pp333-358.

16. Manolagas SC: Birth and death of bone cells: basic regulatory mechanisms and implications for the pathogenesis and treatment of osteoporosis. Endocr Rev 21: 115-137, 2000.

17. Manolagas SC, Weinstein RS, Bellido T, Bodenner DL: Opposite effects of estrogen on the life span of osteoblasts / osteocytes vs. ostoclasts in vivo and in vitro: an explanation of the imbalance between formation and resorption in estrogen deficiency. J Bone Miner Res 14: S169, 1999.

18. Orwoll ES, Klein RF: Osteoporosis in men. Endocr Rev 16: 87-116, 1995.

19. Parfitt AM, Mundy GR, Roodman GD, Hughes DE, Boyce BF : A new model for the regulation of bone resorption, with particular reference to the effects of bisphosphonates. J Bone Miner Res 11: 150-159, 1996.

20. Sims NA, Gooi JH: Bone remodeling: multiple cellular interactions required for coupling of bone formation and resorption. Semin Cell Dev Biol 19: 444-451, 2008.

21. Toribatake Y, Hutton WC, Tomita K, Boden SD: Vascularization of the fusion mass in a posterolateral intertransverse process fusion. Spine (Phila Pa 1976) 23: 1149-1154, 1998.

22. Chao EY, Inoue N, Koo TK, Kim YH. Biomechanical considerations of fracture treatment and bone quality maintenance in elderly patients and patients with osteoporosis. ClinOrthop Relat Res.12-25. 2004.

23. Melton, L.J., 3rd, et al., Perspective. How many women have osteoporosis? J Bone Miner Res, 1992. **7**(9): p. 1005-10.

24. Eastell, R., et al., Classification of vertebral fractures. J Bone Miner Res, 1991. 6(3): p. 207-15.

25. Cummings, S.R. and L.J. Melton, Epidemiology and outcomes of osteoporotic fractures. Lancet, 2002. 359(9319): p. 1761-7.

26. Gabriel, S.E., et al., Direct medical costs attributable to osteoporotic fractures. Osteoporos Int, 2002. 13(4): p. 323-30.

27. Crisan M, Yap S, Casteilla L et al. A perivascular origin for mesenchymal stem cells in multiple human organs. Cell Stem Cell 2008; 3:301-313

28. Crisan M, Huard J, Zheng B, et al. Purification and culture of human blood vessel-associated progenitor cells. Curr Protoc Stem Cell Biol. 2008 Chapter 2: Unit 2B.2.1–2B.2.13.

29. Crisan M, Deasy B, Gavina M, et al. Purification and long-term culture of multipotent progenitor cells affiliated with the walls of human blood vessels: Myoendothelial cells and pericytes. Methods Cell Biol.2008; 86:295–309.

30. Corselli M, Chen CW, Crisan M, et al. Perivascular ancestors of adult multipotent stem cells. Arterioscler Thromb Vasc Biol. 2010; 30:1104–1109.

31. Chen CW, Montelatici E, Crisan M, et al. Perivascular multi-lineage progenitor cells in human organs: Regenerative units, cytokine sources or both? Cytokine Growth Factor Rev. 2009; 20:429–434.

32. Crisan M, Chen CW, Corselli M, et al. Perivascular multipotent progenitor cells in human organs. Ann NY Acad Sci. 2009; 1176:118–123.

33. Corselli M, Chen CW, Sun B, et al. The tunica adventitia of human arteries and veins as a source of mesenchymal stem cells. Stem Cells Dev. 2012; 21:1299–1308.

34. Levi B, Wan DC, Glotzbach JP, et al. CD105 protein depletion enhances human adipose-derived stromal cell osteogenesis through reduction of transforming growth factor beta1 (TGF-beta1) signaling. J Biol Chem.2011; 286:39497–39509.

35. Jiang T, Liu W, Lv X, et al. Potent in vitro chondrogenesis of CD105 enriched human adipose-derived stem cells. Biomaterials. 2010; 31:3564–3571.

36. Gimble JM, Zvonic S, Floyd ZE, Kassem M, Nuttall ME. Playing with bone and fat. J Cell Biochem.98:251-66. 2006.

37. Dominguez LJ, Di Bella G, Belvedere M, Barbagallo M. Physiology of the aging bone and mechanisms of action of bisphosphonates. Biogerontology.12:397-408.

38. Takeshita S, Fumoto T, Naoe Y, Ikeda K, et al. Age related adipogenesis is linked to increased expression of RANKL. J Biol Chem. 2014 Jun 13:289(24):16699-710.

39. Zipfel GJ, Guiot BH, Fessler RG: Bone grafting. Neurosurg Focus 14: e8, 2003.

40. Sung Bae Park, Chun Kee Chung, et al. Strategies of Spinal Fusion on Osteoporotic Spine. J Korean Neurosurg Soc 49**:** 317-322, 2011.

41. Zhang X, Zara J, Siu RK et al. The role of NELL-1, a growth factor associated with craniosynostosis, in promoting bone regeneration. Journal of dental research. 2010;89:865-878.

42. Kwak J, Zara JN, Chiang M et al. NELL-1 injection maintains long-bone quantity and quality in an ovariectomy-induced osteoporotic senile rat model. Tissue engineering Part A. 2013;19:426-436.

43. Askarinam A, James AW, Zara JN et al. Human perivascular stem cells show enhanced osteogenesis and vasculogenesis with Nel-like molecule I protein. Tissue engineering Part A.

2013;19:1386-1397.

44. Chung CG, James AW, Asatrian G et al. Human perivascular stem cell-based bone graft substitute induces rat spinal fusion. Stem cells translational medicine. 2014;3:1231 1241.

45. Vaccaro AR, Chiba K, Heller JG, et al. Bone grafting alternatives in spinal surgery. Spine J. 2002 May-Jun; 2(3):206-15.

46. Laurencin C, Khan Y. Bone Graft Substitute Materials. emedicine 2004. [Accessed February 16, 2012].

47. Laurie SW, Kaban LB, Mulliken JB, et al. Donor-site morbidity after harvesting rib and iliac bone. Plast Reconstr Surg. 1984; 73:933–938.

48. Frodel JL, Jr., Marentette LJ, Quatela VC, et al. Calvarial bone graft harvest. Techniques, considerations, and morbidity. Arch Otolaryngol Head Neck Surg. 1993; 119:17–23.

49. Meliga E, Strem BM, Duckers HJ, et al. Adipose-derived cells. Cell Transplant. 2007; 16:963–970.

50. De Ugarte DA, Morizono K, Elbarbary A, et al. Comparison of multi-lineage cells from human adipose tissue and bone marrow. Cells Tissues Organs. 2003; 174:101–109.

51. Aust L, Devlin B, Foster SJ, et al. Yield of human adipose-derived adult stem cells from liposuction aspirates. Cytotherapy. 2004; 6:7–14.

52. Sandhu HS, Grewal HS, Parvatanei H. Bone grafting for spinal fusion. Orthop Clin North Am. 1999 Oct; 30(4): 685-98.

53. Park SB, Park SH, Kim NH et al. BMP-2 induced early bone formation in spine fusion using rat ovariectomy osteoporosis model. The spine journal : official journal of the North American Spine Society. 2013;13:1273-1280.

54. Li W, Lee M, Whang J et al. Delivery of lyophilized Nell-1 in a rat spinal fusion model. Tissue engineering Part A. 2010;16:2861-2870.

55. Parfitt AM, Drezner MK, Glorieux FH et al. Bone histomorphometry: Standardization of nomenclature, symbols, and units. J Bone Miner Res 1987; 2:595–610.

56. Jee WS, Yao W. Overview: animal models of osteopenia and osteoporosis. J Musculoskelet Neuronal Interact.1:193-207. 2001.

57. Aghaloo T, Jiang X, Soo C et al. A study of the role of nell-1 gene modified goat bone marrow stromal cells in promoting new bone formation. Mol Ther 2007; 15:1872–1880.

58. Kawamoto T, Kawamoto K. Preparation of thin frozen sections from nonfixed and undecalcified hard tissues using Kawamot's film method (2012). Methods Mol Biol 2014; 1130:149–164.

59. Cortet B. Bone repair in osteoporotic bone: Postmenopausal and cortisone-induced osteoporosis. Osteoporosis Int 2011; 22: 2007–2010.

60. Takahata M, Ito M, Abe Y et al. The effect of anti-resorptive therapies on bone graft healing in an ovariectomized rat spinal arthrodesis model. Bone 2008; 43:1057–1066.

61. Nakao S, Minamide A, Kawakami M et al. The influence of alendronate on spine fusion in an osteoporotic animal model. Spine 2011; 36:1446–1452.

62. Moazzaz P, Gupta MC, Gilotra MM et al. Estrogen-dependent actions of bone morphogenetic Morphogenetic protein-7 on spine fusion in rats. Spine 2005; 30: 1706–1711.

63. Lu J, Bhargav D, Wei AQ et al. Posterolateral intertransverse spinal fusion possible in osteoporotic rats with BMP-7 in a higher dose delivered on a composite carrier. Spine 2008; 33: 242–249.

64. Park SB, Park SH, Kang YK et al. The time-dependent effect of ibandronate on bone graft remodeling in an ovariectomized rat spinal arthrodesis model. Spine J 2014; 14:1748–1757.

65. James AW, Pan A, Chiang M et al. A new function of Nell-1 protein in repressing adipogenic differentiation. Biochem Biophys Res Commun 2011; 411:126–131.

66. Zhang X, Peault B, Chen W et al. The Nell-1 growth factor stimulates bone formation by purified human perivascular cells. Tissue Eng Part A 2011; 17:2497–2509.

67. Shen J, James AW, Zara JN et al. BMP2- induced inflammation can be suppressed by the osteoinductive growth factor NELL-1. Tissue Eng Part A 2013; 19: 2390–2401.

68. James AW, Shen J, Zhang X et al. NELL-1 in the treatment of osteoporotic bone loss. Nature communications 2015; 6:7362.

69. Cuomo AV, Virk M, Petrigliano F et al. Mesenchymal stem cell concentration and bone repair: Potential pitfalls from bench to bedside. J Bone Joint Surg Am Vol 2009; 91: 1073–1083.

70. Chen HT, Lee MJ, Chen CH et al. Proliferation and differentiation potential of human adipose-derived mesenchymal stem cells isolated from elderly patients with osteoporotic fractures. J Cell Mol Med 2012; 16:582–593.

71. Moerman EJ, Teng K, Lipschitz DA et al. Aging activates adipogenic and suppresses osteogenic programs in mesenchymal marrow stroma/stem cells: The role of PPAR-gamma2 transcription factor and TGF-beta/BMP signaling pathways. Aging Cell 2004; 3:379–389.

72. Gad SC. Pharmaceutical Manufacturing Handbook: Regulations and Quality. Hoboken, NJ: John Wiley and Sons, 2008.

73. Dahl JA, Duggal S, Coulston N et al. Genetic and epigenetic instability of human bone marrow mesenchymal stem cells expanded in autologous serum or fetal bovine serum. Int J Dev Biol 2008; 52:1033-1042.

74. Constantino PD, Freidman CD. Synthetic bone graft substitutes. Otolaryngol Clin North Am 1994; 27:1037—73.

75. Cypher TJ, Grossman JP. Biological principles of bone graft healing. J Foot Ankle Surg 1996; 35:413—7.

76. Giannoudis PV, Dinopoulos H, Tsiridis E. Bone substitutes: An update. Injury, Int. J. Care Injured (2005) 36S, S20-S27.

77. Bruder SP, Kraus KH, Goldberg VM, Kadiyala S. The effect of implants loaded with autologous mesenchymal stem cells on the healing of canine segmental bone defects. J Bone Joint Surg Am 1998; 80:985—96.

78. Kon E, Muraglia A, Corsi A, et al. Autologous bone marrow stromal cells loaded onto porous hydroxyapatite ceramic accelerate bone repair in critical-size defects of sheep long bones. J Biomed Mater Res 2000; 49:328—37.

79. Gazdag AR, Lane JM, Glaser D, Forster RA. Alternatives to autogenous bone graft: efficacy and indications. J Am Acad Orthop Surg 1995; 3:1—8.

80. Pittenger MF, Mackay AM, Beck SC, et al. Multilineage potential of adult human mesenchymal stem cells. Science 1999; 284: 143-147.

81. Lennon DP, Haynesworth SE, Bruder SP, et al. Human and animal mesenchymal progenitor cells from bone marrow: Identification of serum for optimal selection and proliferation. In Vitro Cell Bio 1996; 32: 602-611.

82. Auquier P, et al. Comparison of anxiety pain and discomfort in two procedures of hematopoietic stem cell collection: Leukacytapheresis and bone marrow harvest. Bone Marrow Transplant 1995; 16: 541-547.

83. Conget PA & Minguell JJ. Phenotypical and functional properties of human bone marrow mesenchymal progenitor cells. Journal of Cellular Physiology 1999; 181: 67-73.

84. Digirolamo CM, Stokes D, Colter D, Phinney DG, Class R & Prockop DJ. Propagation and senescence of human marrow stromal cells in culture: a simple colony-forming assay identifies samples with the greatest potential to propagate and differentiate. British Journal of Haematology 1999; 107: 275-281.

85. Mitchell JB, McIntosh K, Zvonic S, et al. The immunophenotype of human adipose-derived cells. Temporal changes in stromal-associated and stem cell-associated markers. STEM CELLS 2006; 24: 376-385.

86. Stenderup K, Justesen J, Eriksen ET, et al. Number and proliferative capacity of osteogenic stem cells are maintained during aging and in patients with osteoporosis. J Bone Miner Res 2001; 16:1120-1129.

87. James A, Zara J. , et al. Perivascular Stem Cells: A Prospectively Purified Mesenchymal Stem Cell Population for Bone Tissue Engineering. Stem Cells Translational Medicine 2012; 510-519.

88. James A, Zara J. , et al. An Abundant Perivascular Source of Stem Cells for Bone Tissue Engineering. Stem Cells Transl Med 2012; 1(9): 673-84.